Event soliton formation in mixed energy-momentum gaps of nonlinear spacetime crystals

Liang Zhang [1], Zhiwei Fan,[2,*] and Yiming Pan [1,†]

[1] *School of Physical Science and Technology and Center for Transformative Science, ShanghaiTech University, Shanghai 200031, China*

[2] *School of Engineering, Newcastle University, Newcastle upon Tyne NE1 7RU, United Kingdom*

(Received 25 March 2025; accepted 4 March 2026; published 1 May 2026)

We report the formation of a soliton—termed "event soliton"—in nonlinear photonic spacetime crystals (STCs). In these media, simultaneous spatiotemporal periodic modulation of the dielectric constant generates mixed frequency (ω) and wave vector (k) gaps. Under Kerr nonlinearity, the event solitons emerge as fully localized entities in both spacetime and energy-momentum domains, providing a tangible demonstration of the concept of "event" in relativity. The ωk-gap mixture arises from the coexistence and competition between time-reflected and Bragg-reflected waves due to the spatiotemporal modulation. We propose a partial differential equation to capture various spatiotemporal patterns and present numerical simulations to validate our theoretical predictions, reflecting a three-way balance among k-gap opening, ω-gap opening, and nonlinearity. Our work opens avenues for fundamental studies and fosters experimental prospects for implementing spacetime crystals and pattern formation in time-varying photonics.

DOI: 10.1103/q226-dkk4

I. INTRODUCTION

Recently, the study of spacetime crystals (STCs) in photonics—also known as spatiotemporal photonic crystals [1] or spacetime metamaterials [2,3]—has garnered widespread interest. Unlike photonic crystals (PhCs) [4] or photonic time crystals (PTCs) [5–15], photonic STCs feature a dielectric constant that varies periodically in both space and time, as described by $\epsilon(x,t) = \epsilon(x+\Lambda, t+T)$, where Λ and T are the spatial and temporal periodicities, respectively. In PhCs, spatial periodicity leads to an energy gap (ω gap) via Bragg reflection [16], while temporal periodicity in PTCs results in a momentum gap (k gap) through time reflection [8,17,18]. STCs support both ω gaps and k gaps, enabling distinctive bandgap engineering (temporal modulation reshapes spatial Bragg bands). Sharabi *et al.* introduced the concept of a "mixed energy-momentum gap" (ωk gap) [1,19], which emerges when these two gaps converge and overlap, thereby yielding mixed ωk-gapped mode dynamics.

In a dispersive medium, wave propagation exhibits frequency-dependent wave vector. For an STC, when the dispersion relation contains a gap (forbidden band), it is more precisely described as a dispersion-dissipation relation [20], as both the frequency and wave vector acquire complex values: the real parts govern dispersion, while the imaginary components represent dissipation. Notably, modes within ω gap or k gap exhibit distinct dissipative behaviors based on the sign of the imaginary parts. For ω-gapped modes, the momentum (or wave vector) is complex, with the imaginary part scaled by the gap size, leading to spatial attenuation under energy conservation, with the unphysical amplifying mode excluded. Conversely, k-gap modes feature complex frequencies whose imaginary parts correspond to the gap size, resulting in exponential growth or decay over time [15,21–23]. It should be noted that this growing mode is physical, in a sense that the system extracts energy from temporal modulation, highlighting a distinction between k-gapped and ω-gapped modes. This property is pivotal for lasing and amplification in PTCs [24,25]. In a spacetime crystal, the coexistence of spatial and temporal periodicities gives rise to both ω and k gaps. When these two bandgaps overlap, they form a mixed energy-momentum gap [see Fig. 1(h)]. Within the mixed gap, the system exhibits spatial and temporal amplification or attenuation simultaneously due to both complex frequencies and wave vectors, thus dictating unstable propagation of ωk-gapped modes.

A key question in this work is whether nonlinear mechanisms can stabilize the mode dissipation within ωk gaps, a possibility that has not yet been reported. In Bragg gratings, nonlinearity generates localized states known as Bragg solitons, which are spatially confined ω-gapped solutions that remain stationary. These gap solitons were extensively studied in the late 1980s [26–33] and can be well characterized by the nonlinear Schrödinger equation (NLSE) in the form of $[(1-\partial_{xx})\psi - 2|\psi|^2\psi = 0]$ [34]. Similarly, nonlinearity in the k-gap region gives rise to temporally localized modes. Notably, the k-gap soliton reported by Pan *et al.* [35] is spatially homogeneous and propagates at a superluminal velocity while preserving Einstein causality, and is accurately modeled by the NLSE as $[(1-\partial_{tt})\psi - 2|\psi|^2\psi = 0]$. This k-gap soliton

*Contact author: zhiwei.fan@newcastle.ac.uk

†Contact author: yiming.pan@shanghaitech.edu.cn

Published by the American Physical Society under the terms of the Creative Commons Attribution 4.0 International license. Further distribution of this work must maintain attribution to the author(s) and the published article's title, journal citation, and DOI.

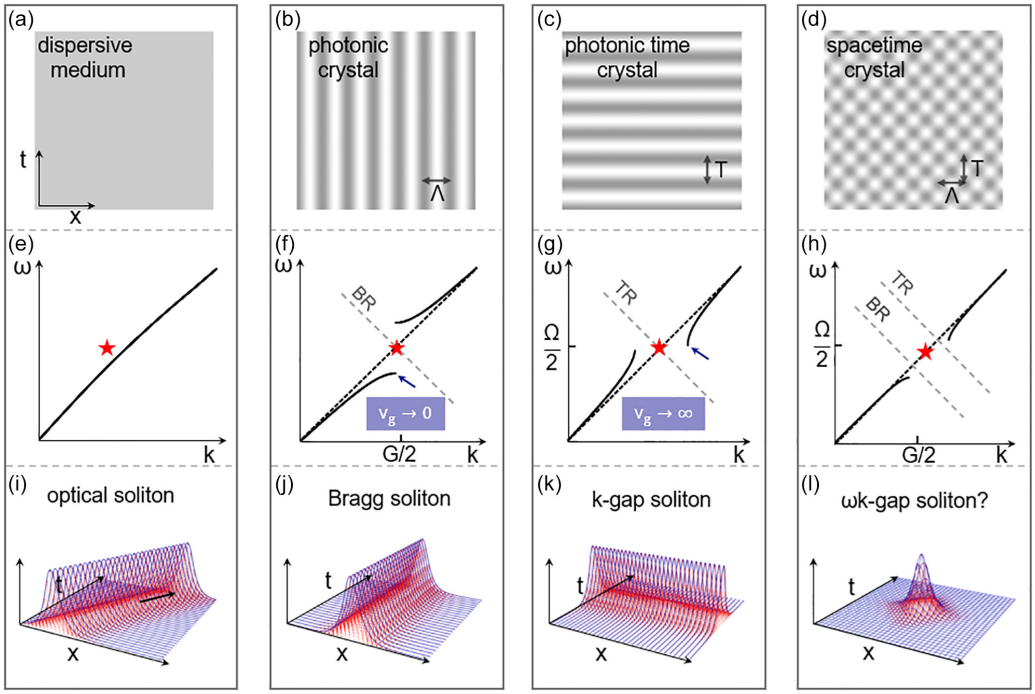


FIG. 1. Schematic comparison of diverse photonic media, band structures, and soliton formations. (a) Dispersive medium. (b) Photonic crystals with spatial modulation. (c) Photonic time crystals with temporal modulation. (d) Spacetime crystals with spatiotemporal modulation. Corresponding band structures: (e) Ordinary dispersion, (f) Energy ω-gapped band due to Bragg reflection (BR), (g) Momentum k-gapped band due to time reflection (TR), and (h) Mixed ωk-gapped band due to both reflections. Kerr nonlinearity is introduced to form gap solitons: (i) traveling soliton, (j) Bragg (ω gap) soliton at zero group velocity, (k) Superluminal k-gap soliton at infinite group velocity, and (l) Eventlike ωk-gap soliton.

exhibits a dual spacetime structure in comparison to the Bragg soliton achieved by substituting the spatial derivative (∂_{xx}) with temporal derivative (∂_{tt}). These gap solitons are compared schematically in Fig. 1.

Here, we hypothesize the presence of an "event soliton" within the mixed ωk gap, exhibiting both spatial and temporal localization, as depicted in Figs. 1(l) and 1(h). To facilitate such a localized solution, without mentioning the specific setting, we intuitively propose a normalized nonlinear wave equation: $(1-\partial_{tt})(1-\partial_{xx})\psi - 4|\psi|^2\psi = 0$. We investigate how Kerr nonlinearity ($|\psi|^2\psi$) enables four unstable ωk-gapped modes to mutually counterbalance, forming an event soliton. This eventlike localization can be interpreted as a nonlinear mixing among the gapped modes, analogous to $\operatorname{sech} x \operatorname{sech} t = 4/(e^{x+t} + e^{-x+t} + e^{-x-t} + e^{x-t})$, displaying spontaneous temporal emergence and spatial indeterminacy. Our hypothesis reveals a nontrivial spatiotemporally localized solution in our setting of a nonlinear STC, where energy and momentum are pinned in the mixed ωk gap, and its dynamics satisfies the newly constructed nonlinear wave equation. Finally, we discuss the implications of our findings for the experimental realization of nonlinear STCs.

II. MODELING

To derive the event soliton and its governing equation as shown in Figs. 1(h) and 1(l), we start by modeling the nonlinear STC depicted in Fig. 1(d). In a nonmagnetic dielectric medium without free charges and moving currents ($\rho = 0, \boldsymbol{J} = 0$), Maxwell's equations in a source-free medium are given by $\nabla \times \boldsymbol{E} = -\frac{\partial \boldsymbol{B}}{\partial t}$, $\nabla \times \boldsymbol{B} = \mu_0 \frac{\partial \boldsymbol{D}}{\partial t}$, with divergence equations $\nabla \cdot \boldsymbol{D} = 0$, $\nabla \cdot \boldsymbol{B} = 0$, where $\boldsymbol{E}$ is the electric field, $\boldsymbol{D}$ is the electric displacement, $\boldsymbol{B}$ is the magnetic field, and μ_0 is the vacuum permeability. Applying the curl operator ($\nabla\times$) to the first equation and substituting the result into the second yields $\frac{\partial^2 \boldsymbol{D}}{\partial t^2} = -\frac{1}{\mu_0}\nabla \times (\nabla \times \boldsymbol{E})$. Assuming a centrosymmetric medium where second-order nonlinearity is negligible, the electric displacement field can be expressed as $D = \epsilon(x,t)E = \epsilon_0(\epsilon_1(x,t) + \chi_3|E|^2)\,E$, where the Kerr nonlinearity χ_3 is dominant. The linear dielectric constant, ϵ_1, is modulated periodically in space and time and is given by $\epsilon_1(x,t) = \epsilon_r\tilde{\epsilon}(x)\tilde{\epsilon}(t) = \epsilon_r(1+\delta_1\cos(\Omega t))(1+\delta_2\cos(Gx))$. Here, ϵ_r is the mean permittivity, and, for weak modulation, the modulation depths $\delta_{1,2}$ are approximately 0.2. $\Omega = 2\pi/T$ and $G = 2\pi/\Lambda$ specify the temporal and spatial modulation frequencies, with periods T and Λ, respectively. In a one-dimensional isotropic medium, the electric field can be reciprocally expressed in terms of the displacement as $E = \frac{D}{\epsilon_0\epsilon_1} - \frac{\chi_3 D^3}{\epsilon_0^2\epsilon_1^4}$, where $\chi_3/\epsilon_0\epsilon_1^4$ denotes the reciprocal third-order nonlinearity [36]. Substituting this into the governing equation yields

$$\frac{\partial^2 D}{\partial t^2} = \frac{1}{\mu_0}\frac{\partial^2}{\partial x^2}\left(\frac{D}{\epsilon_0\epsilon_1} - \frac{\chi_3 D^3}{\epsilon_0^2\epsilon_1^4}\right). \tag{1}$$

In time-varying media, the electric displacement $D$is favored over the electric field Ebecause D remains continuous across temporal boundaries, as dictated by Gauss's law ($\nabla \cdot \boldsymbol{D} = 0$), whereas E may be discontinuous [37].

These temporal boundaries give rise to phenomena such as time reflection and time refraction [18]. For small modulation amplitudes $\delta_{1,2} \ll 1$ and weak nonlinearity χ_3, Eq. (1) can be simplified to $\frac{(1+\delta_2\cos Gx)}{c^2}\frac{\partial^2\tilde{E}}{\partial t^2} = (1-\delta_1\cos\Omega t)\frac{\partial^2\tilde{E}}{\partial x^2} - \beta|\tilde{E}|^2\frac{\partial^2\tilde{E}}{\partial x^2}$, where $\tilde{E} = D/\tilde{\epsilon}(x)$ is the reduced electric displacement and $c = c_0/\sqrt{\epsilon_r} = c_0/n_0$ is the speed of light in the medium, with $n_0 = \sqrt{\epsilon_r}$ being the refractive index and c_0 the light speed in vacuum. We approximate $\tilde{\epsilon}^{-1}(t) = 1 - \delta_1\cos\Omega t$ and focus on the self-phase-modulation term in the nonlinearity by redefining the Kerr coefficient $\beta = 3\chi_3/\epsilon_0\epsilon_r^3$. This nonlinear modulated wave function encapsulates the modulated electromagnetic waves in the nonlinear STC and serves as the base model for our analysis.

To derive the event soliton, we further simplify it to nonlinear coupled-mode equations [38], based on the Floquet-Bloch theorem. To seek Floquet-Bloch waves as the sum of spatiotemporally modulated forward and backward waves, we assume $\tilde{E}(x,t) = A_f e^{i\frac{G}{2}x - i\frac{\Omega}{2}t} + A_b e^{-i\frac{G}{2}x - i\frac{\Omega}{2}t} + A_f^* e^{-i\frac{G}{2}x + i\frac{\Omega}{2}t} + A_b^* e^{i\frac{G}{2}x + i\frac{\Omega}{2}t}$. Accordingly, we may choose that a light pulse with carrier wavelength of 800 nm requires a spatial modulation with period of $\Lambda = 400$ nm and a temporal modulation with period of $T = 1.3$ fs for the setting of a photonic spacetime crystal, corresponds to a modulation frequency $\Omega = 2\pi/T \approx 770$ THz, i.e., comparable to optical carrier frequencies. A_f and A_b in ansatz are the complex amplitudes of the forward- and backward-propagating waves, and their conjugates A_f^* and A_b^*. Substituting the ansatz into nonlinear modulated wave function and applying the slowly varying envelope approximation ($\delta_{1,2} \ll 1$, $\beta \ll 1$) yields the coupled-mode equations:

$$
\begin{aligned}
iG\frac{\partial A_f}{\partial x} + i\frac{\Omega}{c^2}\frac{\partial A_f}{\partial t} + \lambda A_f + \kappa_1 A_b^* + \kappa_2 A_b &= \gamma(|A_f|^2 + 2|A_b|^2)A_f,\\
-iG\frac{\partial A_b}{\partial x} + i\frac{\Omega}{c^2}\frac{\partial A_b}{\partial t} + \lambda A_b + \kappa_1 A_f^* + \kappa_2 A_f &= \gamma(2|A_f|^2 + |A_b|^2)A_b,\\
-iG\frac{\partial A_f^*}{\partial x} - i\frac{\Omega}{c^2}\frac{\partial A_f^*}{\partial t} + \lambda A_f^* + \kappa_1 A_b + \kappa_2 A_b^* &= \gamma(|A_f|^2 + 2|A_b|^2)A_f^*,\\
iG\frac{\partial A_b^*}{\partial x} - i\frac{\Omega}{c^2}\frac{\partial A_b^*}{\partial t} + \lambda A_b^* + \kappa_1 A_f + \kappa_2 A_f^* &= \gamma(2|A_f|^2 + |A_b|^2)A_b^*.
\end{aligned}
\tag{2}
$$

Here, $\lambda = (\Omega^2/c^2 - G^2)/4$ represents the mismatch between temporal and spatial modulation frequencies. The coupling strengths are given by $\kappa_1 = \delta_1 G^2/8$, $\kappa_2 = \delta_2\Omega^2/8c^2$, and the nonlinear coefficient is $\gamma = -3\beta G^2/4$. These equations capture the scattering between Floquet-Bloch waves, including Bragg reflection ($A_f \leftrightarrow A_b$) and time reflection ($A_f \leftrightarrow A_b^*$). The decomposition into forward- and backward-propagating waves reveals self-phase modulation and cross-phase modulation terms arising from the nonlinear mixing.

III. MIXING THE ENERGY AND MOMENTUM GAPS

To derive the ωk-gapped dispersion, we rewrite the Floquet-Bloch waves as a spinor with four components $\psi = (A_f, A_b, A_f^*, A_b^*)^T$. Equation (2) can be recast in a compact form

$$
\left(G\left(i\frac{\partial}{\partial x}\right)\sigma_z\tau_z + \frac{\Omega}{c^2}\left(i\frac{\partial}{\partial t}\right)\sigma_z\tau_0 + \lambda\sigma_0\tau_0 + \kappa_1\sigma_x\tau_x + \kappa_2\sigma_0\tau_x - \gamma\mathcal{L}_{\mathrm{NL}}[\psi]\right)\psi = 0, \tag{3}
$$

where σ_i, τ_j are Pauli operators, with $\sigma_i\tau_j = \sigma_i \otimes \tau_j$ for $i, j = 0, x, y, z$. The nonlinear term $\mathcal{L}_{\mathrm{NL}}[\psi] = |A_f|^2\sigma_0(3\tau_0 - \tau_z)/2 + |A_b|^2\sigma_0(3\tau_0 + \tau_z)/2$ accounts for both self-phase and cross-phase modulations. To obtain the band structure associated with the linear part of Eq. (3), we consider plane-wave solutions of the form $\psi = \chi e^{iPx - iEt}$, where χ is a spinor, with P being the effective wave vector and E the effective frequency. By suppressing the nonlinear term ($\gamma = 0$), the resulting band structure for the coupled modes is

$$
\left((PG)^2 - \left(\frac{E\Omega}{c_r^2}\right)^2 - \lambda^2 - \kappa_1^2 + \kappa_2^2\right)^2 = 4\left(\frac{E\Omega\lambda}{c_r^2}\right)^2 + 4(\lambda\kappa_1)^2. \tag{4}
$$

Figure 2 illustrates the band structure engineering of the forward-propagating wave in the STCs. Details are provided in Sec. 2 of the Supplemental Material [39]. We define the modulation ratio $r = \Omega/Gc$ as a control parameter, so that the mismatch $\lambda = G^2(r^2 - 1)/4$. Without loss of generality, we hold G constant and set the same modulation amplitudes $\delta_1 = \delta_2 = \delta$ (notice that still $\kappa_1 \neq \kappa_2$). By altering Ω (corresponding to$r$), the band structure can be engineered to maintain the fixed energy ω gap while bringing the momentum k gap closer to it. For $r \ll 1$ [Fig. 2(a)], the ω gap and k gap remain well separated. The complex wave vectors are confined within the ω gap and the complex frequencies reside in the k gap, appearing in pairs. At the bandgap edges, the group velocity of the ω gap is zero, whereas for the k gap, it is infinite.

As the ratio$r$ increases to 0.85 [Fig. 2(b)], the k gap draws critically closer to the ω gap. By $r = 0.95$, the two gaps merge into a single mixed gap (the so-called ωk gap), where both frequency and wave vector become simultaneously complex. At this point, the lower branch band edge exhibits infinite group velocity $v_g^{(-)} \to \infty$, and the upper branch has zero group

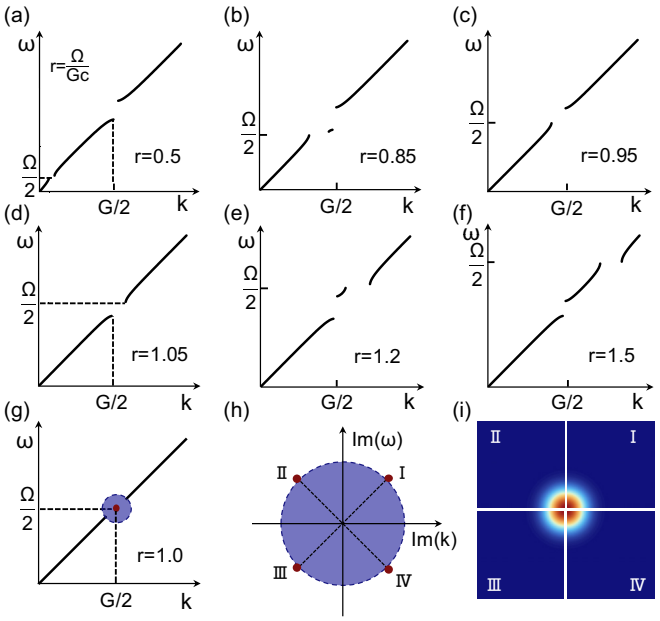


FIG. 2. Band structure engineering and ωk-gapped modes of a photonic spacetime crystal. We tune the modulation ratio $r = \Omega/Gc_r$. (a)–(f) As r increases, the k gap progressively approaches the energy gap, forming a mixed energy-momentum gap before separating again at higher ratios. In panel (g) when $r = 1$, the light-cone modulation causes all ωk-gapped modes to collapse to a fixed frequency and wave vector $(\Omega/2,\ G/2)$, while its imaginary parts build up a dissipation relation in panel (h). The spatiotemporal patterns of these gapped modes are plotted in panel (i), corresponding to red points in panel (h).

velocity $v_g^{(+)} \to 0$. When r slightly surpasses 1, the mixed ωk gap persists, but the group velocities at the band edges interchange, resulting in $v_g^{(-)} \to 0$ and $v_g^{(+)} \to \infty$. Within the ωk gap, four gapped modes emerge, displaying simultaneous amplification or attenuation in spacetime, leading to complex unstable patterns. Increasing r further, for example, to 1.2 [Fig. 2(e)] or 1.5 [Fig. 2(f)], leads to the reseparation of the k gap from ω gap.

In the bandgap engineering, an intriguing phenomenon occurs at $r = 1$ [Fig. 2(g)], termed "light-cone modulation." At this ratio, these ωk-gapped modes converge such that their real parts collapse to the modulation center $(G/2, \Omega/2)$ in the band. However, the imaginary parts of the frequency and wave vector emerge to build up a dissipation relation around the center, given by $\mathrm{Im}(\omega)^2 = \mathrm{Im}(k)^2$, as shown in Fig. 2(h). Notably, the plane-wave solution $\psi = \chi e^{iPx-iEt}$ becomes invalid for describing these gapped modes. Instead, we introduce a dissipative ansatz $\psi' = \chi e^{\xi x-\eta t}$, where η, ξ are assumed to be real, corresponding to the imaginary parts of the frequency and wave vector. At the center ($r = 1$), the linear dissipation relation $|\eta| = c|\xi|$ holds (see Fig. S2 in the Supplemental Material) [39]. As shown in Fig. 2(i), four degenerate dissipative modes emerge: $\chi_m e^{\eta t-\xi x}$, $\chi_m e^{\eta t+\xi x}$, $\chi_m e^{-\eta t+\xi x}$, and $\chi_m e^{-\eta t-\xi x}$, where $m = a, b, c, d$ denote the mode indices. These dissipative modes determine the possible spatiotemporal behavior and pattern formation within the ωk gaps when the nonlinearity ($\mathcal{L}_{\mathrm{NL}}[\psi]$) is considered.

IV. SOLITON FORMATION IN THE MIXED ωk-GAP

Under light-cone modulation, the gapped eigenmode spinors are $\chi_a = (-\mathrm{i}, \mathrm{i}, -\mathrm{i}, \mathrm{i})^T/2$, $\chi_b = (\mathrm{i}, -\mathrm{i}, -\mathrm{i}, \mathrm{i})^T/2$, $\chi_c = (-1, -1, 1, 1)^T/2$, $\chi_d = (1, 1, 1, 1)^T/2$, respectively. In our analysis, we seek spatiotemporally localized solutions of the form $\psi = a(x,t)\chi e^{iP_0x-iE_0t}$, where $P_0^2 = E_0^2/c^2$, and at the modulation center $P_0 = 0$, $E_0 = 0$. By selecting one of these spinors, χ_d, and setting $\lambda = 0$ and $\kappa_1 = \kappa_2 = \kappa$, we substitute the ansatz into Eq. (3), yielding a differential equation for the slowly varying amplitude $a(x,t)$, given by

$$\left(1 - \frac{\Omega^2}{4\kappa^2 c_r^4}\frac{\partial^2}{\partial t^2}\right)\left(1 - \frac{G^2}{4\kappa^2}\frac{\partial^2}{\partial x^2}\right)a - \frac{3\gamma}{8\kappa}|a|^2 a = 0, \quad (5)$$

which admits an analytical solution in the ωk gap, $a = \frac{4\sqrt{2\kappa}}{\sqrt{3\gamma}}\mathrm{sech}(\frac{2\kappa c^2}{\Omega}t)\mathrm{sech}(\frac{2\kappa}{G}x)$. Accordingly, the electric displacement D is then given by

$$D(x,t) = \frac{8\sqrt{2\kappa}}{\sqrt{3\gamma}}(1 + \delta_2 \cos Gx)\mathrm{sech}\left(\frac{2\kappa c^2 t}{\Omega}\right)\mathrm{sech}\left(\frac{2\kappa x}{G}\right) \times \cos\left(\frac{Gx}{2}\right)\cos\left(\frac{\Omega t}{2}\right). \quad (6)$$

The detailed derivation of this equation from χ_d can be found in Sec. 5 in the Supplemental Material [39]. Equation (6) demonstrates a dual-localized structure in time and space arising from a delicate nonlinear mixing of the four ωk-gapped modes. This nonlinear mixing aligns with strategies observed in Bragg soliton and k-gap soliton formation, extending similar principles into the spacetime domain. Full derivations are provided in the Supplemental Material [39].

This event soliton [Eq. (6)] is one of our key achievements in this work, with the following features: the peak intensity scales proportionally with the modulation strength (κ) and is inversely proportional to the nonlinearity (γ), oscillating with a frequency half of the temporal modulation and a wave vector half of the spatial modulation. The ωk-gap soliton is called an event soliton due to simultaneous localization in spatiotemporal and energy-momentum domains, analogous to a classical event in special relativity. The wave-packet size of event soliton is determined by the ωk-gap size, indicating a constraint imposed by the uncertainty principle.

V. GENERATING SPATIOTEMPORAL PATTERNS FROM A LOCALIZED INPUT

To numerically explore the general behavior, we simplify the nonlinear wave equation [Eq. (5)] to a normalized partial differential equation:

$$(1 - \partial_{tt})(1 - \partial_{xx})\psi - 4|\psi|^2\psi = 0, \quad (7)$$

where time t, space x, and field ψ are dimensionless variables renormalized from Eq. (5). A direct check confirms the normal form of event soliton: $\psi = \mathrm{sech}\, x\, \mathrm{sech}\, t$. Under specific constraints, Eq. (7) can further yield k-gap solitons or Bragg solitons. For instance, assuming spatial independence $\partial_{xx}\psi = 0$, Eq. (7) reduces to $(1 - \partial_{tt})\psi - 4|\psi|^2\psi = 0$, which admits a k-gap soliton solution $\psi = \frac{1}{\sqrt{2}}\mathrm{sech}\, t$. On the other hand, when the solution becomes temporally independent $\partial_{tt}\psi = 0$,

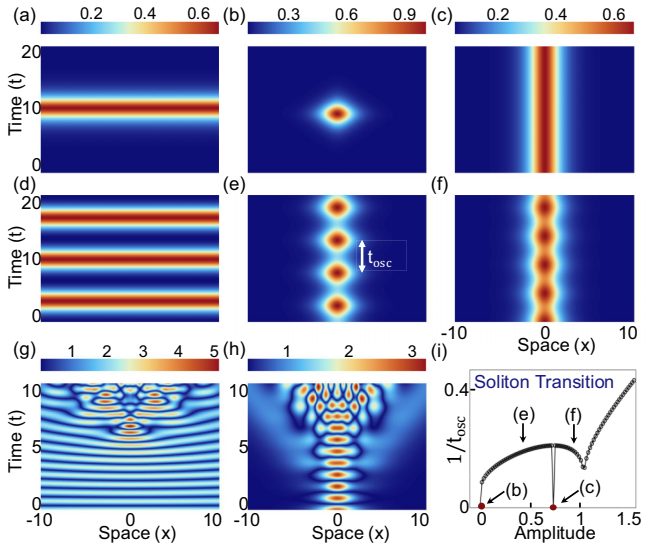


FIG. 3. Numerical analysis of spatiotemporal pattern formations in nonlinear STCs. Evolution of fundamental gap solitons: (a) k gap, (b) event, and (c) Bragg solitons. Multiple and high-order soliton generations: (d) multiple k gap, (e) multiple event, and (f) high-order Bragg solitons. (g), (h) Emergence of event solitons from imperfect initial conditions. (i) Transition between event and Bragg solitons by increasing the input amplitude, illustrating a conversion pathway from event, high-order Bragg to high-order event solitons.

Eq. (7) simplifies to $(1-\partial_{xx})\psi - 4|\psi|^2\psi = 0$, yielding the Bragg soliton solution $\psi = \frac{1}{\sqrt{2}}\operatorname{sech} x$. Additionally, in the absence of the nonlinear term when $(1-\partial_{tt})(1-\partial_{xx})\psi = 0$, we obtain analytical solutions $\psi = e^{\pm x \pm t}, e^{\pm x \mp t}$, corresponding to the four ωk-gapped modes [Fig. 2(i)].

We systematically studied Eq. (7) that governs event solitons in spacetime crystals. We found that different spatiotemporal patterns emerge depending on initial conditions. A low-amplitude plane wave with the homogeneous initial condition $\psi(x, 0) = 0.0001$ is used, exponential amplification occurs due to the ωk gap, which eventually triggers nonlinearity and forms a k-gap soliton. As shown in Fig. 3(a), this soliton remains finite in time but extends as a plane wave in space, reflecting a two-way balance between nonlinearity and k-gap opening. Increasing the input plane-wave amplitude leads to higher-order k-gap soliton formation [Fig. 3(d)]. Conversely, when the system is initialized with a localized wave packet (e.g., $A_0 \operatorname{sech} x$) at a small amplitude ($A_0 = 0.0005/\sqrt{2}$), an event soliton forms, fully confined in both space and time [Fig. 3(b)]. A higher input amplitude yields higher-order event solitons [Fig. 3(e)], and when the amplitude reaches exactly $1/\sqrt{2}$, the event soliton transitions to a Bragg soliton, spatially confined and unaffected by k-gap amplification [Fig. 3(c)]. Further increases in amplitude generate higher-order Bragg solitons [Fig. 3(f)]. Notably, unlike the balance required for the formation of k-gap soliton, Bragg soliton requires a balance between nonlinearity and ω-gap opening, while the event soliton results from a three-way balance. For detailed calculations and stability analysis of event solitons, please refer to Secs. 6 and 7 in the Supplemental Material [39].

Figure 3(i) illustrates the transition among soliton formations, revealing a rich conversion pathway: from event soliton to higher-order event solitons, followed by Bragg soliton, high-order Bragg solitons, and back to higher-order event solitons at even higher input amplitudes. Adjusting the width of the input seed introduces additional complexity, enabling spatiotemporal patterns such as imperfect event solitons emerging from high-order k-gap solitons, as depicted in Fig. 3(g). Furthermore, the superluminal characteristics inherent to the k gap are evident in Fig. 3(h), highlighting the diverse nonlinear phenomena accessible in STCs. Overall, these findings elucidate how the interplay of initial amplitude, spatial localization, and wave packet width governs the emergence, instablities, and transitions of spatiotemporal pattern formations [23,40].

VI. FURTHER DISCUSSIONS

Unlike Peregrine soliton [41–44], a spatiotemporal localization that emerges from a weak fluctuation on a nonzero background, the event soliton does not require a continuous background. However, both soliton types can exhibit high amplitudes in spacetime, seemingly materializing abruptly and vanishing without a trace. Compared to the light bullet, a three-dimensional spatiotemporally localized electromagnetic wave proposed in the 1990s [45,46] that conserves energy during propagation as a light pulse, the event soliton manifests as a transient event that cannot be tracked along a continuous timeline.

While photonic spacetime crystals have been extensively studied from various perspectives, their practical realization remains challenging. At radio frequencies, momentum bandgap has been experimentally observed using dynamic transmission lines [47,48]. At optical frequencies, creating photonic time crystals requires high-intensity pump beams to induce periodic refractive-index changes [49], a process constrained by small nonlinear susceptibilities and the impracticality of generating pulse trains with extremely high repetition rates. In our STC setting, the representative parameter is chosen as $\mathrm{T} = 1.3\,\mathrm{fs}$, corresponding to a modulation frequency $\Omega \approx 770\,\mathrm{THz}$, which is comparable to optical carrier frequencies and far beyond conventional electro-optic modulation bandwidths (typically GHz to sub-THz) [50]. Epsilon-near-zero materials [51–54] may overcome these limitations in the foreseeable future. Meanwhile, on two-dimensional metamaterial platforms, modulating surface boundaries can simultaneously amplify both surface and free-space modes [55], suggesting that such spacetime metamaterials could demonstrate momentum bandgap features or the k-gap amplification. Recently, a topological event was reported in time-varying metamaterial [56]. Importantly, similar ωk-gap physics is expected to persist at substantially lower frequencies, provided that the corresponding normalized coupling, dispersion, and nonlinearity can be engineered. For realizing event solitons, modulating surface microwaves using electronic components appears to be a feasible approach within metamaterial STCs.

Noted that in conventional media, solitons are highly susceptible to material dissipation, as even weak losses inhibit their formation. In contrast, the k-gap amplification

mechanism in our nonlinear spacetime crystal compensates for modest loss, though excessive dissipation eventually suppresses the effect. Intrinsic dispersion contributes only perturbatively; instead, the spatiotemporal modulation reshapes the bandgap edges. Although the nonlinear coefficients and bandgap engineering vary with the specific material platform and modulation parameters, the governing model and stability criteria derived here remain applicable.

VII. CONCLUSION

In this work, we introduce the concept of an event soliton in nonlinear photonic spacetime crystals, characterized by spatial confinement and temporal transience, reminiscent of an "event" in special relativity. Crucially, we scrutinized how these solitons emerge from mixed energy-momentum gaps, thereby integrating the previously distinct frameworks of Bragg and k-gap soliton formation. Moreover, the existence of an event soliton implies a broader range of spatiotemporal instabilities and pattern formations in systems with spacetime periodicity. While our findings open avenues for research, several aspects remain unexplored, including higher-order event solitons, multisoliton interactions, and collision dynamics. At this stage, we believe our work lays the groundwork for elucidating the physics of ωk gaps, and stimulates further research in time-varying photonics, spacetime metamaterials, and related fields.

ACKNOWLEDGMENTS

We thank the discussions with Prof. D. Skryabin. Y.P. acknowledges the support of the NSFC (No. 2023X0201-417-03) and the fund of the ShanghaiTech University (start-up funding).

The authors declare no competing financial interests.

DATA AVAILABILITY

No data were created or analyzed in this study.

[1] Y. Sharabi, A. Dikopoltsev, E. Lustig, Y. Lumer, and M. Segev, Spatiotemporal photonic crystals, Optica **9**, 585 (2022).

[2] C. Caloz and Z.-L. Deck-Léger, Spacetime metamaterials—Part I: General concepts, IEEE Trans. Antennas Propag. **68**, 1569 (2019).

[3] C. Caloz and Z.-L. Deck-Leger, Spacetime metamaterials—Part II: Theory and applications, IEEE Trans. Antennas Propag. **68**, 1583 (2019).

[4] E. Yablonovitch, Inhibited spontaneous emission in solid-state physics and electronics, Phys. Rev. Lett. **58**, 2059 (1987).

[5] F. R. Morgenthaler, Velocity modulation of electromagnetic waves, IRE Trans. Microwave Theory Tech. **6**, 167 (1958).

[6] D. Holberg and K. Kunz, Parametric properties of fields in a slab of time-varying permittivity, IEEE Trans. Antennas Propag. **14**, 183 (1966).

[7] J. R. Zurita-Sánchez, P. Halevi, and J. C. Cervantes-Gonzalez, Reflection and transmission of a wave incident on a slab with a time-periodic dielectric function $\epsilon(t)$, Phys. Rev. A **79**, 053821 (2009).

[8] A. M. Shaltout, J. Fang, A. V. Kildishev, and V. M. Shalaev, Photonic time-crystals and momentum band-gaps, in *Conference on Lasers and Electro-Optics*, OSA Technical Digest (online) (Optica Publishing Group, 2016), paper FM1D.4.

[9] J. S. Martínez-Romero and P. Halevi, Parametric resonances in a temporal photonic crystal slab, Phys. Rev. A **98**, 053852 (2018).

[10] N. Wang, Z.-Q. Zhang, and C. T. Chan, Photonic Floquet media with a complex time-periodic permittivity, Phys. Rev. B **98**, 085142 (2018).

[11] J. S. Martínez-Romero, O. M. Becerra-Fuentes, and P. Halevi, Temporal photonic crystals with modulations of both permittivity and permeability, Phys. Rev. A **93**, 063813 (2016).

[12] E. Galiffi, R. Tirole, S. Yin, H. Li, S. Vezzoli, P. A. Huidobro, M. G. Silveirinha, R. Sapienza, A. Alù, and J. B. Pendry, Photonics of time-varying media, Adv. Photon. **4**, 14002 (2022).

[13] Z. Hayran, J. B. Khurgin, and F. Monticone, $\hbar\omega$ versus $\hbar k$: Dispersion and energy constraints on time-varying photonic materials and time crystals, Opt. Mater. Express **12**, 3904 (2022).

[14] H. Moussa, G. Xu, S. Yin, E. Galiffi, Y. Ra'di, and A. Alù, Observation of temporal reflection and broadband frequency translation at photonic time interfaces, Nat. Phys. **19**, 863 (2023).

[15] S. Sadhukhan and S. Ghosh, Momentum controlled optical pulse amplification in photonic time crystals, arXiv:2301.09390.

[16] M. Xiao, Z. Q. Zhang, and C. T. Chan, Surface impedance and bulk band geometric phases in one-dimensional systems, Phys. Rev. X **4**, 021017 (2014).

[17] M. Baggioli, M. Vasin, V. Brazhkin, and K. Trachenko, Gapped momentum states, Phys. Rep. **865**, 1 (2020).

[18] J. T. Mendonça and P. K. Shukla, Time refraction and time reflection: Two basic concepts, Phys. Scr. **65**, 160 (2002).

[19] O. Shahriar and M. R. C. Mahdy, An idea of implementing photonic space-time crystals using metasurfaces, arXiv:2409.00139.

[20] J. W. Thomas, Dispersion and dissipation, in *Numerical Partial Differential Equations: Finite Difference Methods*, Texts in Applied Mathematics Vol. 22 (Springer, New York, NY, 1995), p. 361.

[21] J. B. Pendry, E. Galiffi, and P. A. Huidobro, Gain mechanism in time-dependent media, Optica **8**, 636 (2021).

[22] Y. Yerin, A. A. Varlamov, R. Felici, and A. Di Carlo, Dielectric properties and plasmon modes of gapped momentum systems of different dimensionality, Phys. Rev. B **108**, 075134 (2023).

[23] E. I. Kiselev, Y. Pan, and N. H. Lindner, Light-controlled terahertz plasmonic time-varying media: Momentum gaps, entangled plasmon pairs, and pulse-induced time reversal, Phys. Rev. B **110**, L241411 (2024).

[24] M. Lyubarov, Y. Lumer, A. Dikopoltsev, E. Lustig, Y. Sharabi, and M. Segev, Amplified emission and lasing in photonic time crystals, Science (1979) **377**, 425 (2022).

[25] A. Dikopoltsev, Y. Sharabi, M. Lyubarov, Y. Lumer, S. Tsesses, E. Lustig, I. Kaminer, and M. Segev, Light emission by free electrons in photonic time-crystals, Proc. Natl. Acad. Sci. USA **119**, e2119705119 (2022).

[26] D. L. Mills and S. E. Trullinger, Gap solitons in nonlinear periodic structures, Phys. Rev. B **36**, 947 (1987).

[27] W. Chen and D. L. Mills, Gap solitons and the nonlinear optical response of superlattices, Phys. Rev. Lett. **58**, 160 (1987).

[28] D. N. Christodoulides and R. I. Joseph, Slow bragg solitons in nonlinear periodic structures, Phys. Rev. Lett. **62**, 1746 (1989).

[29] B. J. Eggleton, R. E. Slusher, C. M. De Sterke, P. A. Krug, and J. E. Sipe, Bragg grating solitons, Phys. Rev. Lett. **76**, 1627 (1996).

[30] W. C. K. Mak, P. L. Chu, and B. A. Malomed, Solitary waves in coupled nonlinear waveguides with Bragg gratings, J. Opt. Soc. Am. B **15**, 1685 (1998).

[31] B. J. Eggleton, C. M. de Sterke, and R. E. Slusher, Bragg solitons in the nonlinear Schrödinger limit: Experiment and theory, J. Opt. Soc. Am. B **16**, 587 (1999).

[32] D. Mandelik, R. Morandotti, J. S. Aitchison, and Y. Silberberg, Gap solitons in waveguide arrays, Phys. Rev. Lett. **92**, 093904 (2004).

[33] A. B. Aceves and S. Wabnitz, Self-induced transparency solitons in nonlinear refractive periodic media, Phys. Lett. A **141**, 37 (1989).

[34] J. E. Sipe and H. G. Winful, Nonlinear Schrödinger solitons in a periodic structure, Opt. Lett. **13**, 132 (1988).

[35] Y. Pan, M.-I. Cohen, and M. Segev, Superluminal k-gap solitons in nonlinear photonic time crystals, Phys. Rev. Lett. **130**, 233801 (2023).

[36] P. D. Drummond and M. Hillery, *The Quantum Theory of Nonlinear Optics* (Cambridge University Press, New York, 2014).

[37] N. Quesada and J. E. Sipe, Why you should not use the electric field to quantize in nonlinear optics, Opt. Lett. **42**, 3443 (2017).

[38] H. Kogelnik and C. V. Shank, Coupled-wave theory of distributed feedback lasers, J. Appl. Phys. **43**, 2327 (1972).

[39] See Supplemental Material at http://link.aps.org/supplemental/10.1103/q226-dkk4 for additional details on the band-structure engineering, the derivation of Eq. (6), and the numerical results.

[40] E. I. Kiselev and Y. Pan, Symmetry breaking and spatiotemporal pattern formation in photonic time crystals, Phys. Rev. A **111**, 053509 (2025).

[41] D. H. Peregrine, Water waves, nonlinear Schrödinger equations and their solutions, ANZIAM J. **25**, 16 (1983).

[42] B. Kibler, J. Fatome, C. Finot, G. Millot, F. Dias, G. Genty, N. Akhmediev, and J. M. Dudley, The Peregrine soliton in nonlinear fibre optics, Nat. Phys. **6**, 790 (2010).

[43] V. I. Shrira and V. V. Geogjaev, What makes the Peregrine soliton so special as a prototype of freak waves? J. Eng. Math. **67**, 11 (2010).

[44] D. R. Solli, C. Ropers, P. Koonath, and B. Jalali, Optical rogue waves, Nature (London) **450**, 1054 (2007).

[45] Y. Silberberg, Collapse of optical pulses, Opt. Lett. **15**, 1282 (1990).

[46] F. W. Wise, Generation of light bullets, Physics **3**, 107 (2010).

[47] J. R. Reyes-Ayona and P. Halevi, Observation of genuine wave vector (k or β) gap in a dynamic transmission line and temporal photonic crystals, Appl. Phys. Lett. **107**, (2015).

[48] J. R. Reyes-Ayona and P. Halevi, Electromagnetic wave propagation in an externally modulated low-pass transmission line, IEEE Trans. Microwave Theory Tech. **64**, 3449 (2016).

[49] E. Lustig, O. Segal, S. Saha, E. Bordo, S. N. Chowdhury, Y. Sharabi, A. Fleischer, A. Boltasseva, O. Cohen, and V. M. Shalaev, Time-refraction optics with single cycle modulation, Nanophotonics **12**, 2221 (2023).

[50] Z. Sun, A. Martinez, and F. Wang, Optical modulators with 2D layered materials, Nat. Photon. **10**, 227 (2016).

[51] R. Maas, J. Parsons, N. Engheta, and A. Polman, Experimental realization of an epsilon-near-zero metamaterial at visible wavelengths, Nat. Photon. **7**, 907 (2013).

[52] D. M. Solis and N. Engheta, A theoretical explanation for enhanced nonlinear response in epsilon-near-zero media, in *2020 Conference on Lasers and Electro-Optics (CLEO)* (IEEE, Piscataway, NJ, 2020), pp. 1–2.

[53] Y. Zhou, M. Z. Alam, M. Karimi, J. Upham, O. Reshef, C. Liu, A. E. Willner, and R. W. Boyd, Broadband frequency translation through time refraction in an epsilon-near-zero material, Nat. Commun. **11**, 2180 (2020).

[54] V. Bruno, S. Vezzoli, C. DeVault, E. Carnemolla, M. Ferrera, A. Boltasseva, V. M. Shalaev, D. Faccio, and M. Clerici, Broad frequency shift of parametric processes in epsilon-near-zero time-varying media, Appl. Sci. **10**, 1318 (2020).

[55] X. Wang, M. S. Mirmoosa, V. S. Asadchy, C. Rockstuhl, S. Fan, and S. A. Tretyakov, Metasurface-based realization of photonic time crystals, Sci. Adv. **9**, eadg7541 (2023).

[56] J. Feis, S. Weidemann, T. Sheppard, H. M. Price, and A. Szameit, Space-time-topological events in photonic quantum walks, Nat. Photon. **19**, 518 (2025).